

Estimation of light interception in research environments: a joint approach using directional light sensors and 3D virtual plants applied to sunflower (*Helianthus annuus*) and *Arabidopsis thaliana* in natural and artificial conditions

Karine Chenu^{A,B,E}, Hervé Rey^C, Jean Dauzat^C, Guilioni Lydie^D and Jérémie Lecœur^D

^AINRA, UMR 759 LEPSE, 2 place Viala, 34060 Montpellier cedex 01, France.

^BDepartment of Primary Industries and Fisheries, APSRU, PO Box 102, Toowoomba, Qld 4350, Australia.

^CCIRAD, UMR botAnique et bioinforMatique de l'Architecture des Plantes, Bd de la Lironde, F – 34398 Montpellier, France.

^DSupAgro, UMR 759 LEPSE, 2 place Viala, 34060 Montpellier cedex 01, France.

^ECorresponding author. Email: karine.chenu@dpi.qld.gov.au

This paper originates from a presentation at the 5th International Workshop on Functional–Structural Plant Models, Napier, New Zealand, November 2007.

Abstract. Light interception is a major factor influencing plant development and biomass production. Several methods have been proposed to determine this variable, but its calculation remains difficult in artificial environments with heterogeneous light. We propose a method that uses 3D virtual plant modelling and directional light characterisation to estimate light interception in highly heterogeneous light environments such as growth chambers and glasshouses. Intercepted light was estimated by coupling an architectural model and a light model for different genotypes of the rosette species *Arabidopsis thaliana* (L.) Heynh and a sunflower crop. The model was applied to plants of contrasting architectures, cultivated in isolation or in canopy, in natural or artificial environments, and under contrasting light conditions. The model gave satisfactory results when compared with observed data and enabled calculation of light interception in situations where direct measurements or classical methods were inefficient, such as young crops, isolated plants or artificial conditions. Furthermore, the model revealed that *A. thaliana* increased its light interception efficiency when shaded. To conclude, the method can be used to calculate intercepted light at organ, plant and plot levels, in natural and artificial environments, and should be useful in the investigation of genotype–environment interactions for plant architecture and light interception efficiency.

Additional keywords: artificial environment, radiative model.

Introduction

Light interception is a major factor in plant development, energy balance and biomass accumulation (e.g. Monteith 1977; Chenu *et al.* 2005). Evidence for strong genetic controls has been found for architectural traits affecting light interception, some of which have already been exploited indirectly through plant breeding for yield (e.g. Debaeke *et al.* 2004; Triboui *et al.* 2004). As the amount of light intercepted by a plant is not directly measurable, several methods have been proposed to estimate this variable. Most existing approaches were developed for uniform canopies in natural light environments, without any shading or reflection from the experimental surroundings. However, many physiological and genetic studies are carried out under artificial conditions, for example, in a glasshouse or a growth chamber (e.g. Granier and Tardieu 1999; Cookson and Granier 2006; Walter *et al.* 2007) where walls, supporting structures and artificial lighting render the light climate heterogeneous. In these environments plants experience

different microclimatic conditions depending on their location, and this might greatly affect their development and physiology (Measures *et al.* 1973; Boonen *et al.* 2002). Thus, spatial variability in light distribution should be taken into account in such experimental designs.

Light interception can be estimated in several ways in terms of plant architecture and light climate. Simple approaches based on plant leaf area have been proposed, such as the approximation of light interception from the product of leaf area by incident radiation (e.g. Granier and Tardieu 1999). Application of the Beer–Lambert law to canopies is the most common method (e.g. Kasanga and Monsi 1954; Varlet-Grancher *et al.* 1989; Rinaldi *et al.* 2003). Here, an extinction coefficient (k) is used to relate leaf area index (LAI) to the fraction of incident light intercepted. The coefficient k corresponds to the efficiency with which a unit of leaf area intercepts the incident light. The higher the value of k , the more efficient the plant leaf area intercepts light. The Beer–Lambert law is reasonably effective

for homogeneous canopies, but does not account for 3D plant geometry and is thus not appropriate to calculate the amount of light intercepted by an organ or by sparse canopies such as orchards or vineyards (Louarn *et al.* 2007). Furthermore, k is typically assumed to be constant for a crop, whereas it actually changes rapidly during early plant growth (Louarn *et al.* 2008) and varies with crop management factors such as density (Dauzat *et al.* 2008). The Beer–Lambert law is also regularly applied with an average k value regardless of radiative conditions and does not account for specific variation in radiative conditions, such as changes in the proportions of direct and diffuse radiation, the impact of sun position or light heterogeneity in artificial environments. A second method to estimating light interception is the mixed model. Developed for orchards and vineyards, this approach uses the Beer–Lambert law on restricted volumes, called voxels by analogy with pixels, where leaves form a homogeneous medium (e.g. Röhrig *et al.* 1999; Sinoquet *et al.* 2001; Louarn *et al.* 2007). This method helps to characterise the light environment in sparse canopies made up of some dense zones of vegetation, but suffers from the same limitations of the Beer–Lambert law concerning light intercepted by individual organs and the heterogeneous radiative conditions of artificial environments. A third method considers plants at the organ level, using 3D virtual plants (Mech and Prusinkiewicz 1996; Sinoquet *et al.* 1998; Barczy *et al.* 2008). In this approach, the light balance is calculated on plant mock-ups (Chelle and Andrieu 1999; Rey *et al.* 2008). This generic approach is time consuming, but is potentially applicable to any type of vegetation. It enables estimation of the light intercepted at organ to canopy levels, throughout plant development, and is suitable for analysing how environmental and genetic variations in plant architecture affect light interception.

In the present study, we propose and evaluate a method based on 3D virtual plant modelling coupled with a light model to estimate light absorption throughout plant development, in both natural and artificial environments. Virtual plants were simulated using the AMAPsim model (Barczy *et al.* 2008), which

reproduced plant growth and development over time. The light balance for these virtual plants was calculated using the MMR light model (Dauzat and Eroy 1997; Dauzat *et al.* 2001, 2008) and a directional characterisation of the light environment. As it is based on dividing the sky hemisphere into sectors, the MMR light model enabled simulations of anisotropic light distributions across the hemisphere. Specific directional light sensors called ‘Turtle light sensors’ were engineered and used to characterise light heterogeneity in terms of intensity and spatial distribution. Field, glasshouse and growth chamber experiments were carried out, with different shading conditions, to: (i) parameterise the AMAPsim architectural model for the simulation of plant growth, development and architecture of genotypes with contrasting architecture in a tall crop species (*Helianthus annuus* L.) and a small rosette species (*Arabidopsis thaliana* L.); (ii) adapt the light MMR model commonly used under natural light conditions to light conditions observed in growth chambers and glasshouses; and (iii) test and compare the AMAPsim–MMR combination with other approaches under such situations.

Materials and methods

The plant measurements carried out in each experimental treatment were used to build 3D virtual plants for genotypes of sunflower (*Helianthus annuus* L.) and *Arabidopsis thaliana* L. using AMAPsim (Figs 1 and 2). Simulations were carried out on a daily basis during the vegetative growth period and were compared with observed data for integrated traits, such as projected plant leaf area or LAI.

The light environment was characterised to: (i) test the extent to which incident light and directional light fluxes varied within the growth chamber and glasshouse; (ii) identify subplots with spatially homogenous incident light (shading nets were added where required) and help design experimental layouts; and (iii) parameterise, run and evaluate the MMR light model. In MMR, the light environment was simulated from either: (i) measurements of incident PAR taken throughout the

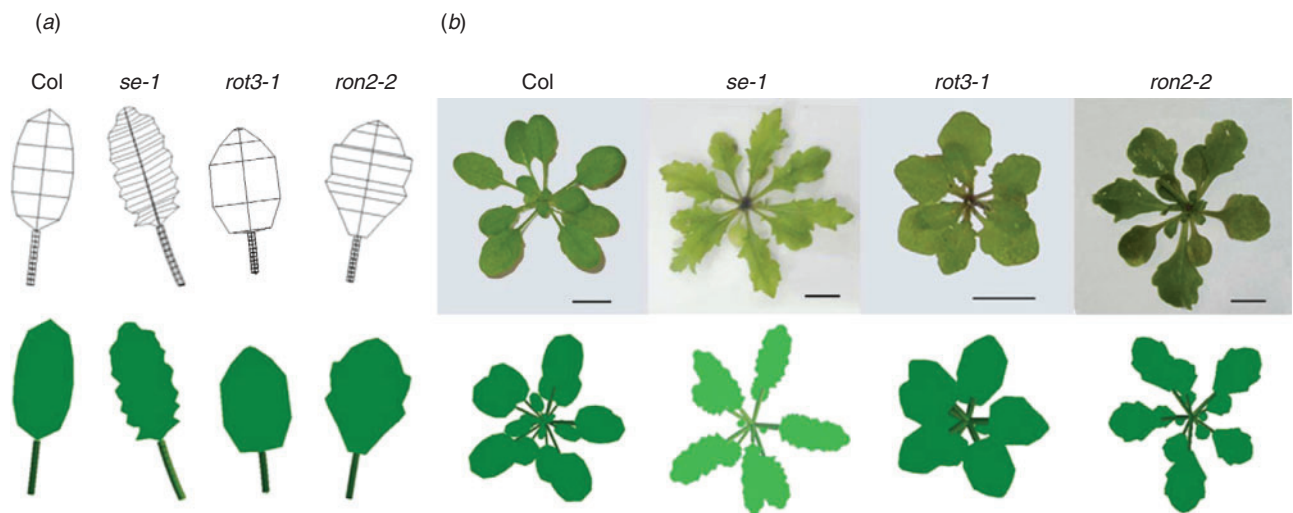


Fig. 1. Representation of (a) virtual leaves and (b) plants for different genotypes of *Arabidopsis thaliana*. (a) Leaf symbols are displayed with skeleton and textured representations. (b) Pictures of a sampled plant and 3D virtual plants corresponding to an averaged representation of the observed plants. From left to right: the ecotype Columbia (Col) and the leaf developmental mutants *se-1*, *rot3-1* and *ron2-2*. Scale bar = 1 cm.

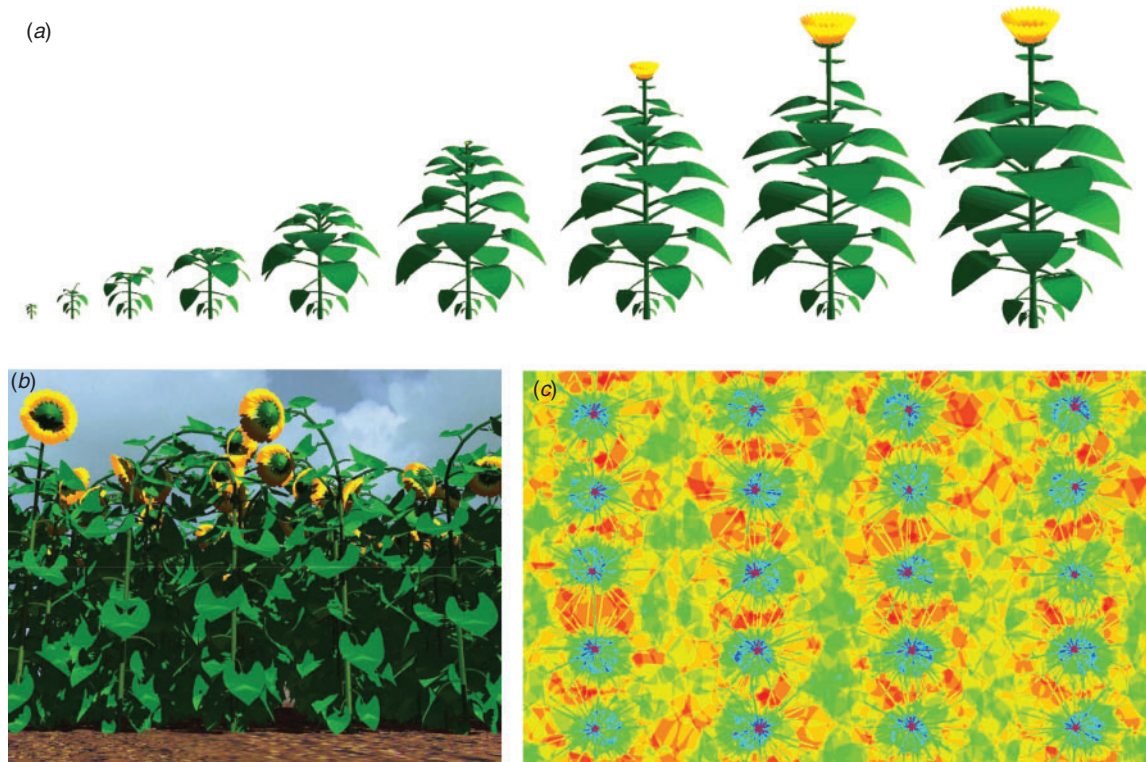


Fig. 2. Representations of 3D virtual plants of sunflower. (a) Albena hybrid, with a 100°Cd (cumulative degree days) growth interval, from 100°Cd to 900°Cd following plant emergence in Experiment S2, (b) virtual plot of the Heliasol hybrid at plant maturity in Experiment S5, and (c) map of the light transmitted at the soil level at the end of all organ expansion, ~1000°Cd after plant emergence.

experiments, field location (longitude and latitude) and time for the field experiments; or (ii) the spatial and temporal characterisation of the directional light fluxes specific to each treatment for the growth chamber and glasshouse experiments. Specific measurements of the fraction of intercepted light were carried out to evaluate the combined model AMAPsim–MMR.

Plant material, experimental design and growth conditions

A. thaliana plants (Fig. 1), ecotypes Columbia (Col-0), Dijon-M (Di-m), Landsberg *erecta* (*Ler*) and Wassilewskija (*Ws*) and their mutants *serrate* (*se-1*; mutant of Col), *rotundifolia* (*rot3-1*; mutant of Col), *rotunda* (*ron2-2*; mutant of *Ler*) and *p70S-KOR* (over-expressor of the *KORRIGANI* gene; mutant of *Ws*) were grown in growth chambers (Conviron E15; Controlled Environments, Winnipeg, Manitoba, Canada) in six experiments (Table 1). Plants were grown in plastic containers (0.5 m wide, 0.2 m long and 0.15 m deep) filled with a mixture (1:1, v/v) of loamy soil and organic compost. Seeds were incubated at 4°C for 3 days and then suspended in water to be sown individually at one seed per cm². Density was reduced twice per week to ensure that the plants did not overlap. Soil water content was maintained at a constant level, close to the soil storage capacity, by daily watering with Hoagland solution (diluted to one-tenth original strength). Light was provided with a 16-h photoperiod in Experiments A1 to A5 and with a 12-h photoperiod in Experiment A6 using a bank of cool-white

fluorescent tubes (neon Slimline F72T12CW; OSRAM Sylvania GmbH, Munich, Germany) and halogen bulbs (100 W Halolux; OSRAM GmbH).

In the sunflower experiments, hybrids Albena and Heliasol (Fig. 2), which have contrasting architectures (Heliasol produces fewer leaves than Albena, has a different leaf area distribution along the stem and has a more flexible stem resulting in upper blending), were grown at Montpellier, southern France (43°40'N, 3°50'E), for five experiments conducted in 1998, 1999 and 2001, in a glasshouse (oriented E–W) and in a field (Table 1). In the glasshouse experiments, the seeds were sown in a 12 m² plot at a density of 2.7 plant m⁻² and at a depth of 3 cm in columns (0.14 m diameter and 0.65 m height) containing a 1:1 mixture (v/v) of loamy soil and organic compost. The soil was maintained at water retention capacity by watering the columns three times per day with a modified, one-tenth strength, Hoagland solution corrected with minor nutrients. Additional light was provided by a bank of sodium lamps maintaining an average photoperiod of 14 h. In the field experiments, the seeds were sown at a depth of 2 cm in a deep sandy loam soil (fluvio-calcaric Cambisol) with 0.60 m row spacing and 0.03 m between the seeds in a row. Plants were grown at a density of 5.6 plants m⁻² along rows oriented N–S, with individual plots for each treatment ranging from 78 to 400 m². Isolated plants were cultivated in the field after a density reduction to 0.06 plant m⁻² at seedling emergence. In all field treatments, nitrogen fertilisation was applied before sowing (80 kg ha⁻¹). The soil water potential was monitored

Table 1. Experimental conditions and characteristics

Mean values for daily incident PAR, atmospheric vapour pressure deficit (VPD) and leaf temperature were calculated from plant emergence to the end of expansion of all leaves. Vapour pressure deficit corresponds to measurements taken during the lighting period. Col, Columbia; Di-m, Dijon-M; *Ler*, Landsberg *erecta*; WS, Wassilewskija; *se-1*, serrate (mutant of Col); *rot3-1*, rotundifolia (mutant of Col); *ron2-2*, rotunda (mutant of *Ler*); *p70S-KOR*, over-expressor of the *KORRIGANI* gene (mutant of WS) *Arabidopsis thaliana*

Sowing date	Experiment #	Species	Genotype	Location	Treatment	Density	Incident PAR (mol m ⁻² day ⁻¹)	VPD (kPa)	Leaf temperature (°C)
24 February 2001	A1	<i>A. thaliana</i>	Col	Growth chamber	Control	–	10.8	0.34	18.4
24 February 2001	A1	<i>A. thaliana</i>	Col	Growth chamber	Moderate shading	–	5.2	0.34	18.6
24 February 2001	A1	<i>A. thaliana</i>	Col	Growth chamber	Severe shading	–	2.5	0.34	18.3
28 May 2001	A2	<i>A. thaliana</i>	Col, Di-m, <i>se-1</i>	Growth chamber	Control	–	9.3	0.71	20.4
28 May 2001	A2	<i>A. thaliana</i>	Col, Di-m, <i>se-1</i>	Growth chamber	Moderate shading	–	6.4	0.71	20.1
28 May 2001	A2	<i>A. thaliana</i>	Col, Di-m, <i>se-1</i>	Growth chamber	Severe shading	–	3.7	0.71	19.9
8 November 2001	A3	<i>A. thaliana</i>	Col, <i>se-1</i>	Growth chamber	Control	–	11.2	0.51	20.3
8 November 2001	A3	<i>A. thaliana</i>	Col, <i>se-1</i>	Growth chamber	Moderate shading	–	5.0	0.51	18.7
8 November 2001	A3	<i>A. thaliana</i>	Col, <i>se-1</i>	Growth chamber	Severe shading	–	3.0	0.51	17.4
24 April 2002	A4	<i>A. thaliana</i>	<i>rot3-1</i>	Growth chamber	Control	–	10.0	0.48	20.8
24 April 2002	A4	<i>A. thaliana</i>	<i>rot3-1</i>	Growth chamber	Moderate shading	–	5.3	0.48	20.5
24 April 2002	A4	<i>A. thaliana</i>	<i>rot3-1</i>	Growth chamber	Severe shading	–	3.2	0.48	17.7
30 July 2002	A5	<i>A. thaliana</i>	<i>Ler</i> , WS	Growth chamber	Control	–	8.3	0.49	20
30 July 2002	A5	<i>A. thaliana</i>	<i>Ler</i> , WS	Growth chamber	Moderate shading	–	4.2	0.49	20.4
30 July 2002	A5	<i>A. thaliana</i>	<i>Ler</i> , WS	Growth chamber	Severe shading	–	2.7	0.49	18.4
12 March 2003	A6	<i>A. thaliana</i>	<i>Ler</i> , WS, <i>rot3-1</i> , <i>ron2-2</i> , <i>p70S-KOR</i>	Growth chamber	Control	–	8.6	0.44	20.4
12 March 2003	A6	<i>A. thaliana</i>	<i>Ler</i> , Di-m, WS, <i>rot3-1</i> , <i>ron2-2</i> , <i>p70S-KOR</i>	Growth chamber	Early shading	–	4.6	0.44	19.8
12 March 2003	A6	<i>A. thaliana</i>	<i>Ler</i> , Di-m, WS, <i>rot3-1</i> , <i>ron2-2</i> , <i>p70S-KOR</i>	Growth chamber	Late shading	–	2.6	0.44	18.2
28 January 1998	S1	Sunflower	Albena	Glasshouse	Control	2.7	20.2	1.79	20.8
5 May 1998	S2	Sunflower	Albena	Field	Isolated plant	0.06	45.7	1.72	22.4
16 October 1998	S3	Sunflower	Albena	Glasshouse	Control	2.7	8.0	1.36	18.8
11 May 1999	S4	Sunflower	Albena	Field	Control	5.6	40.7	1.40	21.1
11 May 1999	S4	Sunflower	Albena	Field	Moderate shading	5.6	10.9 ^A	1.24	20.2
11 May 1999	S4	Sunflower	Albena	Field	Severe shading	5.6	11.1 ^A	1.16	20.8
11 May 1999	S4	Sunflower	Albena	Field	Isolated plant	0.06	51.4	1.40	21.8
5 May 2001	S5	Sunflower	Albena, Heliasol	Field	Control	5.6	55.8	1.27	22.2

^ADuring the shade period.

by five tensiometers (DTE 1000 system; Nardeux, Saint-Avertin, France) placed every 0.20 m at depths of 0.30–1.10 m. The soil water potential was maintained by irrigation above -40 kPa in the top 0.5 m of soil over the period of leaf area establishment to avoid any reduction in stomatal conductance or leaf growth (Sadras and Milroy 1996).

Light treatments

In the experiments *A. thaliana*, the growth chamber was divided into three subplots, and shading nets (cloth #13; Bouillon, Paris, France) were positioned to vary the level of incident radiation and to ensure that incident PAR was spatially homogeneous at the plant level. The plants in each subplot were subjected to a specific light treatment (Table 1): (i) 'control' treatments with light intensity exceeding $7.5 \text{ mol m}^{-2} \text{ day}^{-1}$ (i.e. $130 \text{ } \mu\text{mol m}^{-2} \text{ s}^{-1}$), corresponding to treatments that do not affect plant leaf expansion (Chenu *et al.* 2005); (ii) 'moderate shading' with light intensity between 6.5 and $4 \text{ mol m}^{-2} \text{ day}^{-1}$ ($70\text{--}113 \text{ } \mu\text{mol m}^{-2} \text{ s}^{-1}$); and (iii) 'severe shading' with light intensity of less than $4 \text{ mol m}^{-2} \text{ day}^{-1}$ ($70 \text{ } \mu\text{mol m}^{-2} \text{ s}^{-1}$).

In the glasshouse, the plants were grown in the central part of the building to minimise light heterogeneity. The light environment was also characterised for another position, at the edge of the glasshouse, close to the building structures, to test the extent to which the light environment was heterogeneous in this building.

In the field, sunflower plants were grown in two 400 m^2 plots under a shading net that intercepted 75% of the incident PAR. The first plot was shaded during the visible expansion of leaves 7 to 13, which corresponded to the lower third of the leaves in the final canopy ('early shading' treatment). The second plot was shaded during the visible expansion of leaves 13 to 19, which corresponded to the middle leaves on the main stem ('late shading' treatment). This latter period finished just after the appearance of the floral bud. In this experiment the plants possessed 31.7 ± 1.1 leaves at maturity.

Environmental measurements

Air temperature and relative humidity were measured using a thermohygrometer (HMP35A; Vaisala Oy, Helsinki, Finland) shaded from incident radiation and positioned at plant height in the growth chamber or 2 m above the soil in the field and in the glasshouse. In each treatment, the leaf temperature was monitored by 3–4 microthermocouples (Cooper–Constantan) in the artificial environments (s.d. lower than 0.72°C over the plant cycle) and by 16 thermocouples in the field experiments (s.d. lower than 0.5°C), positioned against the leaf abaxial surface. Incident light was measured using a PAR sensor (LI-190SB; Li-Cor, Lincoln, NE, USA) above the plants. Measurements were taken every 10–20 s and then averaged and stored every 600 s using a datalogger (CR10X; Campbell Scientific, Shephed, UK). The environmental conditions are described in Table 1.

The fraction of intercepted PAR was measured twice per week in field Experiment S5 using a LAI-2000 plant canopy analyser device (Li-Cor), following the procedure for row crops (Anonymous 1992). Each measurement was the average of 12 replicates at various places in the plot. The principle of this

device is based on the use of gap fractions measured by a hemispherical optical sensor that divides the 2π steradians of the sky hemisphere into five portions. Each portion corresponds to a 'ring' with a given range of zenithal elevations where the sky and the canopy are distinguished using a monochromatic sensor (plant components are displayed in black and the sky in white). The gap fraction of each portion is calculated as the portion of the sky hemisphere that is not occulted by plant components and through which incident light can reach the soil. These gap fractions are then integrated to calculate the fraction of incident light reaching the ground (see Jonckheere *et al.* 2004 for more details). These measurements were used to test the AMAPsim–MMR model and to estimate the extinction coefficient (k) of the Beer–Lambert law for the Albena and Heliasol hybrids.

Characterisation of the light environments

To investigate the variability of incident light in artificial environments, the spatial distribution of incident PAR was measured in the growth chamber (with and without the shading net) and in two glasshouse plots (one at the edge of the building to test the extent to which incident light can vary within a small plot, and one in the center of the building, where light heterogeneity was minimal, and where the experiments were undertaken). Measurements were carried out using a $0.125 \text{ m} \times 0.50 \text{ m}$ and $0.13 \text{ m} \times 0.2 \text{ m}$ grid in the growth chamber and the glasshouse plots, respectively. The measurements were made at the soil level in the *A. thaliana* experiments, and at a height of 0.5 m (soil level) and at the top of the mature plants in the glasshouse sunflower experiments.

The directional light fluxes were characterised using two 'Turtle light sensor' devices specifically designed for the present study (Fig. 3). These devices comprise PAR sensors oriented to measure light from different portions of the sky hemisphere. Built according to the den Dulk model (den Dulk 1989), the devices were made of pentagonal or hexagonal sensors that had equal solid angles and were oriented to cover the entire sky hemisphere without overlapping. The first 'Turtle light sensor', called Turtle_16, was built from 16 individual PAR sensors for the field experiments (Fig. 3a). A smaller 'Turtle light sensor' device (less than 0.1 m across), called Turtle_6, was built for the artificial environments and had five lateral faces with a 26.57° elevation and one top horizontal sensor (Fig. 3b). In the field, measurements with Turtle_16 were made at a height of 2 m in the middle of the trial over the experimental period (in accordance with meteorological standards). In the growth chamber, measurements were taken using Turtle_6 at the plant level using a $0.15 \times 0.30 \text{ m}$ grid at the start and end of each experiment (because light provided by the lamps was constant during the lighting period). In the glasshouse, a specific procedure was developed because the light changed over time, and measurements with Turtle_6 were not taken continually throughout the experiments. The interaction between natural light and the glasshouse structures was taken into account by means of directional transmission coefficients (t). These coefficients corresponded to the fraction of external light penetrating into the glasshouse in a given direction over a day,

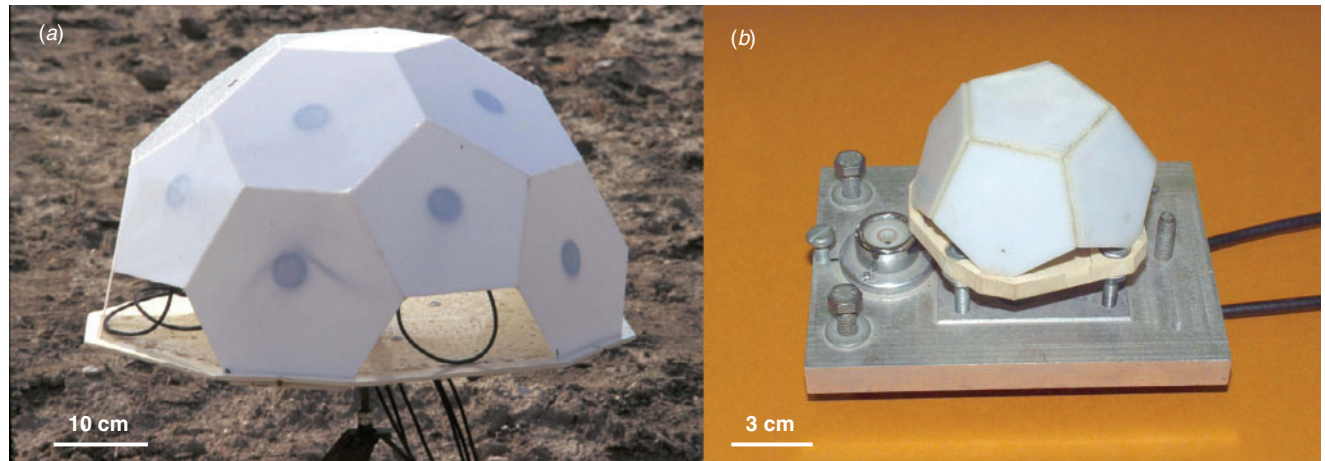


Fig. 3. Pictures of the 'Turtle light sensor' devices that were used to characterise the directional light environment. (a) The Turtle₁₆ was built from 16 individual PAR sensors for the field experiments, while (b) a smaller device called Turtle₆ was built with only six faces for the growth chamber and glasshouse experiments.

and were estimated from the differences between Turtle₆ measurements taken inside and outside the glasshouse. The t coefficients were assumed to be constant over the entire experimental period because they mainly depended on the characteristics of the building structures. The coefficients were estimated just before the start of each experiment over 10–15 consecutive days, thus encompassing a broad range of light intensities and compositions (direct *v.* diffuse light). Artificial light provided by the lamps was measured during the night using the Turtle₆. Overall, the light available to plants was estimated for each direction as the sum of the light coming in from outside ($t \times PAR_{\text{outside}}$) and the artificial light from lamps over the lighting period. These measurements were used in the MMR light model to simulate directional light fluxes.

Plant measurements

In the *A. thaliana* experiments, samples of six plants were harvested every 2–3 days over the first 10 days after plant emergence and then every 3–4 days until the end of rosette expansion. The plants were dissected under a microscope (Leica wild F8Z stereomicroscope; Leica, Wetzlar, Germany) connected to a video camera (CCD-IRIS/RGB colour video camera; Sony, Tokyo, Japan). The blade area of each leaf in the harvested plants was determined using an image analyser (Bioscan-Optimas V4.10, Edmonds, WA, USA). The lengths and widths of the blades and petioles were measured in one sample out of two. Phyllotaxy and zenithal angles were measured once per week with a digital protractor (Pro 360, Travers, NY, USA).

In the sunflower experiments, non-destructive measurements were carried out on eight to 10 median plants selected in each plot on the basis of stem diameter and plant height. Destructive samples were taken three times per week from four to six plants at a similar development stage from plant emergence to capitulum initiation. These plants were dissected under a microscope and the number and area of the leaves enclosed in the apical bud were measured as described for *A. thaliana*. Non-destructive measurements were carried out three times per week from plant emergence to cessation of all organ expansion

(~70 days after plant emergence). Plant height, stem diameter, internode and petiole length and diameter, blade length and width (length > 1 mm) were measured using a ruler and digital callipers (0.1 mm), with an average error of 0.01 m for plant height and 1 mm for stem diameter and blade, internode and petiole dimension. The angles of phyllotaxy, petiole insertion on stem, petiole and blade flexion and rotation were measured with a protractor (Pro 360). Blade shape was studied to ensure that there was no difference with position on the stem, and that blade area could be estimated from measurements of only length and width. A highly significant linear relationship ($r^2 > 0.99$, $n > 300$, $P < 0.001$) was established in each experiment between the product of length by width and the previously measured blade area.

Leaf growth and development variables

Variables related to phytomer development were expressed in relation to thermal time (cumulative degree days ($^{\circ}\text{Cd}$)), making it possible to account for differences in temperatures between experiments and treatments (Table 1). Daily thermal time was calculated as the difference between the daily mean leaf temperature and a base temperature of 3°C for *A. thaliana* and 4.8°C for sunflower (Granier and Tardieu 1998; Granier *et al.* 2002).

Plant emergence was defined as the date on which the first leaf was initiated (0.001 mm^2) in *A. thaliana*, and the date on which the first leaf pair became visible (3–5 mm in length) between open cotyledons in sunflower.

The timing of phytomer initiation was estimated by a linear relationship between the number of phytomers initiated and thermal time. Phytomers were considered initiated when their primordia reached 0.001 mm^2 in *A. thaliana* and 0.04 mm in sunflower, which corresponded, respectively, to the minimum leaf size observable under a microscope and to the length of the youngest leaf primordia.

The change in thermal time since organ initiation (tt) was calculated for blade length and width, internode and petiole length and stem diameter in sunflower, and for blade area in *A. thaliana*

(Y), for each phytomer and each experimental situation as follows (Lecoeur and Ney 2003):

$$Y = \frac{Y_f}{1 + \exp\left(4 ER_m \frac{t_m - t}{Y_f}\right)}, \quad (1)$$

where Y_f corresponds to 97% of the final dimension of the considered organ, and ER_m and t_m are fitted parameters corresponding, respectively, to the maximum expansion rate of the organ and the thermal time at which this maximal expansion rate occurred.

In sunflower, blade area was estimated from blade length and width, as previously described. In *A. thaliana*, petiole length (L_{petiole}) and width (W_{petiole}) were estimated in relation to the blade area (A) of the considered leaf:

$$L_{\text{petiole}} = a + b A^c, \quad (2)$$

$$W_{\text{petiole}} = d + e \ln(A), \quad (3)$$

where a , b , c , d and e are fitted parameters estimated for each experimental situation.

Three-dimensional virtual plants

Three-dimensional virtual plants (Figs 1 and 2) were generated to reproduce sunflower and *A. thaliana* plants on a daily basis, and in each treatment, using the AMAPsim program (Chenu *et al.* 2005, 2007; Barczi *et al.* 2008; Rey *et al.* 2008; for a detailed description see <http://amap.cirad.fr>). Plant topology and organ geometry were specific to each species. Genotype geometry differed only for blade shape in *A. thaliana* (Fig. 2) and for organ orientation and twisting in sunflower. Blades of *A. thaliana* were considered to be flat, whereas in the sunflower blade curvature, winglet elevation and bending of the blade distal part were reproduced. Blade shape in both *A. thaliana* and sunflower varied with leaf rank and with experimental treatment, and was simulated based on observed data for the ratio between blade length and width. Blades were simulated by symbols made up of 8–46 polygons depending on species and genotype. Phyllotaxy was considered to be stable over time and experimental situation. Zenithal angles for the different phytomers decreased over time, following the pattern observed. Organ orientation and bending for sunflower plants in the canopy were estimated in relation to distribution based on measurements taken for five plants in each treatment. Thus, single plants in the simulated sunflower canopy differed in terms of geometry.

Organ growth and development on the virtual plants were particular to each experimental condition. The timing of phytomer initiation was calculated from observed data, as previously described. Leaf blades expanded in response to temperature, following Eqn (1). Petiole length and width were estimated from Eqn (1) in sunflower and Eqns (2) and (3) in *A. thaliana*. Internode expansion was nil in *A. thaliana* and estimated from Eqn (1) in sunflower. Phytomer initiation and organ growth were established from observed data on an average plant, meaning that all plants in a plot had organs of the same size in both *A. thaliana* and sunflower.

Virtual plots

LANDMAKER software (Auclair *et al.* 2001) was used to monitor plant positions in a virtual plot in relation to the plant design of each situation. The 3D virtual *A. thaliana* plants were positioned in the middle of a 0.1×0.1 m virtual plot. Virtual sunflower plants grown in canopy were positioned in a 3.2 m² plot, every 0.6×0.3 m in the field or every 0.6×0.6 m in the glasshouse, with small random variations accounting for the observed deviations from theoretical positions. Isolated sunflower plants were positioned in the middle of a 16 m² plot. Seedlings were azimuthally oriented at random. Plots were virtually duplicated to the infinity in all directions using the toricity option of the MMR model, such that radiative simulations were carried out without border effects.

Light balance

The generated 3D virtual plants were used to estimate plant radiative balance in each light treatment. The radiative climate in the virtual plots was estimated by the MMR model (Dauzat and Eroy 1997; Dauzat *et al.* 2008) for short waves (400–700 nm). This model considers incident light as a set of directional light fluxes spread over the sky hemisphere (den Dulk 1989). In the field, 46 directional light fluxes were calculated from incident light (using a horizontal PAR sensor), field location (longitude and latitude) and time (Dauzat *et al.* 2001). Measurements carried out with the Turtle_16 device were solely used to evaluate model accuracy in field situations for 16 of these 46 directional light fluxes. In the glasshouse and growth chamber, only six directions of light fluxes were used as input into the model (considering six instead of 46 directions led to 6% differences in the simulations in the field). The six directional light fluxes incoming from the sky sectors were calculated by inverting the measurements carried out with the Turtle_6 device for each treatment. The measured irradiation of each sensor i (I_i) was expressed as a function of the six incident fluxes (F) oriented along the normals (N) of the Turtle_6 device:

$$I_i = \sum_{n=1}^6 (N_i \cdot N_n) F_n, \quad (4)$$

where F_n corresponds to the flux density in the direction normal to the sensor n and $N_i \cdot N_n$ is the dot product between the normals of the sensors i and n , respectively ($N_i \cdot N_n$ is set to zero for angles between N_i and N_n that were larger than $\pi/2$ because the sensors only receive light from a single hemisphere).

The MMR computer programs simulate the radiative transfers within layers of the canopy in three steps, as follows. For each sky sector, the first module, *Mir*, calculated the interception of the directional light by the soil and the vegetation elements (each polygon of the internodes, petioles, blades and the capitulum) proportionally to the number of their pixels visible in the considered direction. The second module, *Musc*, then calculated the multiple scattering of the intercepted light within each layer and the resulting additional irradiation of vegetation and soil. *Musc* processed exchanges of scattered radiation between horizontal layers, for each direction. To reduce computation time, the total scattered light intercepted was distributed among vegetation constituents proportionally

to their area, within each layer. The two complementary modules *Mir* and *Musc* provided a detailed light balance of the canopy for each illumination direction. Finally, the third module, *Radbal*, combined the outputs of the previous modules to obtain the complete light balance of the plot for the light environment of the experimental situation considered. Organ irradiance was finally obtained as the sum of partial irradiances by incident (calculated for each of its polygons) and scattered (calculated at the scale of the vegetation layer) light received from each sky sector.

Radiative variables

The fraction of PAR intercepted by the canopy (ϵ_i) was calculated from the daily incident PAR above the canopy ($PAR_{incident}$) and the daily incident PAR at the soil level ($PAR_{incident(soil)}$):

$$\epsilon_i = \frac{PAR_{incident} - PAR_{incident(soil)}}{PAR_{incident}} \quad (5)$$

According to this definition, ϵ_i depicts only the interception of incident radiation and does not account for scattered radiation. Measurements of the fraction of intercepted PAR were carried out using the LAI-2000, based on the gap fraction, which also did not account for scattered radiation.

Conversely, the calculation of PAR absorbed by a plant organ includes its interception of incident PAR ($PAR_{i(organ)}$) plus the additional fraction of light scattered by vegetation and soil, and intercepted by the organ ($PAR_{s(organ)}$). Thus, the daily PAR absorbed by an organ ($PAR_{a(organ)}$) is given by:

$$PAR_{a(organ)} = (PAR_{i(organ)} + PAR_{s(organ)}) * (1 - \rho - \tau), \quad (6)$$

where ρ and τ are the reflection and transmission coefficients determined for the PAR range, respectively. Reflectances of 0.15, 0.12 and 0.18 were measured for sunflower blades, *A. thaliana* blades and soil, respectively, using a spectroradiometer (Fieldspec; ASD, Arvada, CO, USA). Blade transmission and reflection coefficients were assumed to be equal for blades (as proposed by Guyot 1990), and independent of blade face. Petioles, sunflower stem and sunflower capitulum (mainly composed of bracts during the period considered) were considered to have the same reflectance as blades, and zero transmittance (as proposed by Guilioni and Lhomme 2006).

Relative leaf irradiance (*RLI*) was calculated to estimate plant light interception efficiency and was thus expressed relative to incident PAR. It was defined as PAR irradiance of the blades ($\text{mol m}_{leaf}^{-2} \text{day}^{-1}$) divided by the product of incident PAR ($\text{mol m}_{ground}^{-2} \text{day}^{-1}$) and plant blade area ($A_{(leaf)}$, m_{leaf}^2):

$$RLI = \frac{\sum(PAR_{i(leaf)} + PAR_{s(leaf)})}{PAR_{incident} * A_{(leaf)}} \quad (7)$$

Statistical analysis

Fitting parameters in the model (inputs) were computed from linear and non-linear adjustments using Table Curve 2D 4.0 (Systat Software, Richmond, CA, USA). Fits of observed and simulated (model outputs) data were evaluated on the basis of their analytical quality by the coefficient of determination (r^2) and their predictive quality by the coefficient of variation of error (CVe), which determines the mean error when using a given

equation and a set of parameters to predict a Y value from an X value. CVe was calculated as follows:

$$CVe = \frac{\sqrt{\sum(y'_i - y_i)^2}}{\sum \frac{y_i}{n}}, \quad (8)$$

where y_i , y'_i and n are the 'observed' and adjusted values and the number of data points, respectively. The CVe numerator is equal to the root mean square of errors (RMSE).

Results

Spatial light distribution in growth chambers and glasshouses is very heterogeneous

Incident PAR was markedly heterogeneous inside the growth chamber (0.8×1.8 m) and on a $3 \text{ m} \times 4 \text{ m}$ surface at the edge of the glasshouse (Fig. 4a–d). Owing to the reflective properties of the walls, incident PAR at the soil level varied by more than 30% in the growth chamber. A greater than 30% variation was also observed for daily incident PAR in the plot at the edge of the glasshouse, where building structures shaded the plants. This heterogeneity was greatly increased when using additional artificial lighting, which generated strong light gradients over a few decimetres.

Based on characterisation of the incident light distribution, subplots were defined within each artificial environment to cluster the light heterogeneity. The spatial variability was further reduced with the addition of shading nets where required. Thus, the growth chamber area was divided into three subplots of $\sim 0.5 \text{ m}^2$, where shading nets were added to adjust the level of incident radiation. The resulting incident light only varied by $\sim 6\%$ within these subplots, and values measured by the lateral sensors of the Turtle_6 device varied by $\sim 10\%$ for a given direction. In the glasshouse, experiments were conducted in a small subplot of the building (12 m^2) positioned near the centre of the building. Within this subplot, daily incident light had a maximum variation of 8% and daily directional light fluxes varied by $\sim 6\%$ for any given direction.

In these subplots, directional light fluxes were nevertheless highly variable across directions. When measurements were taken in the growth chamber without shading, as well as after adding fine-meshed netting to homogenise incident light (control treatment), light measured with the Turtle_6 lateral sensors varied between 40 and 70% of incident light (measured vertically), depending on the direction considered (Fig. 4e). The addition of darker shading nets allowed us to obtain homogenous, low-incident light (moderate and severe shading treatments), but the nets affected directional light fluxes: the normalised light flux (ratio between lateral and vertical incident light) either decreased or increased depending on the direction considered (Fig. 4e). In the centre of the glasshouse, external light was reduced from 20 to 80% by the windows and building structures before reaching the plants (Fig. 4f), depending on the direction considered. Artificial light from lamps also modified the directional light fluxes received by the plants (Fig. 4f).

A detailed characterisation of the directional light environment in which the plants were grown was used by MMR to reproduce *in silico* a similar environment over time

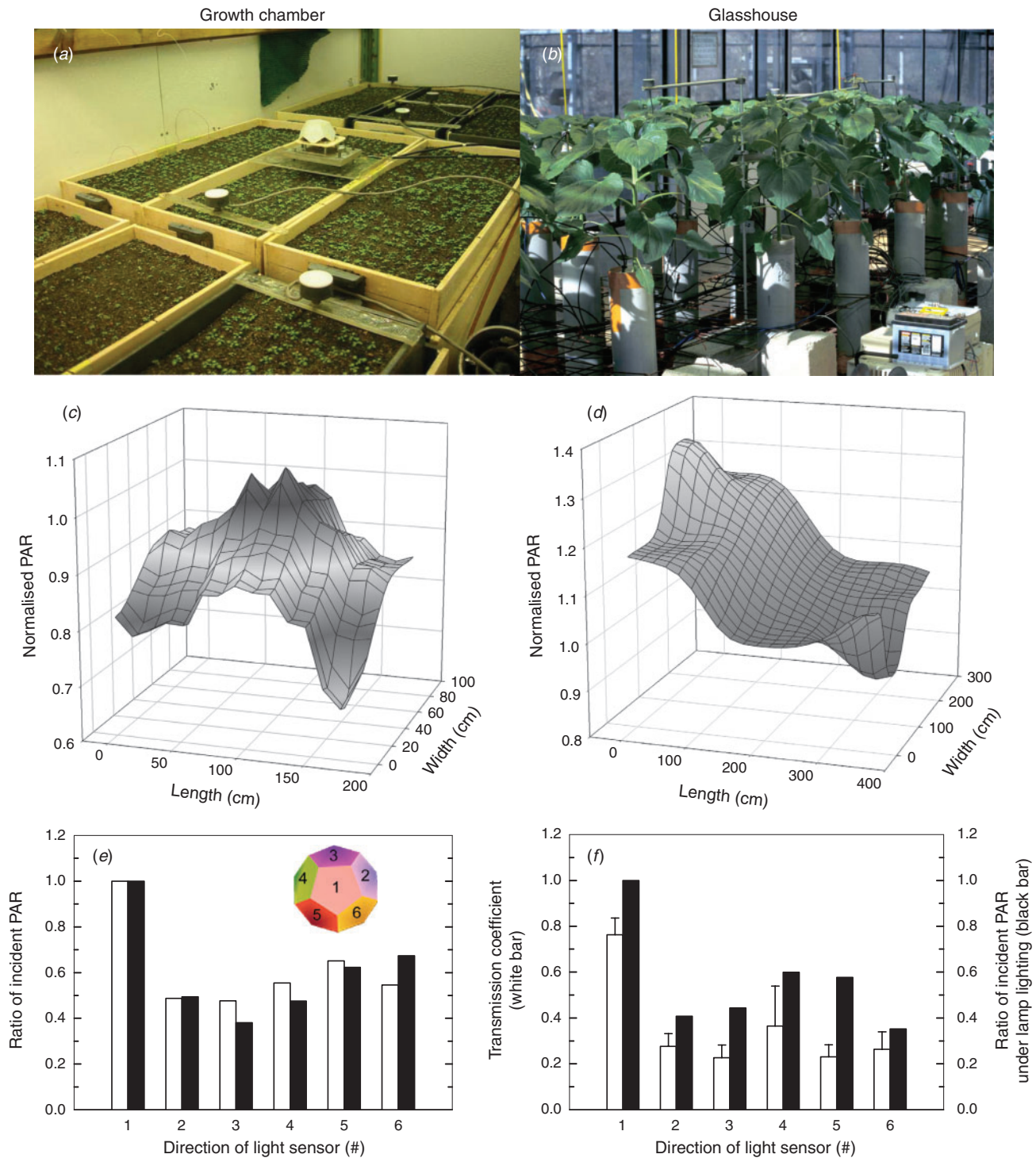


Fig. 4. (a, b) Picture, (c, d) example of the spatial distribution of incident light and (e, f) lateral light for different directions in (a, c, e) the growth chamber and (b, d, f) the glasshouse. (c, d) Spatial mapping of incident PAR at the soil level normalised for incident PAR measured in (c) the growth chamber and (d) a 12 m² plot at the edge of the greenhouse. These data (c, d) illustrate the large variability that can be found within the growth chamber and the greenhouse. To avoid heterogeneity problems, experiments were conducted in locations where light heterogeneity was minimal (12 m² plot located in the middle of the greenhouse and 1.5 m² subplots covered by shading nets in the growth chamber). (e) Relative PAR values of lateral light from different directions (see inset) measured with Turtle_6 sensors (ratio of PAR for sector #*i* over incident PAR measured by the horizontal, top sector (#1)) at a given position in the growth chamber in the absence (white bar) or presence (black bar) of shading nets. (f) Coefficient of light transmission (transmission coefficient = internal PAR/external PAR) measured in the centre of the glasshouse for the six directions over 1-day periods without additional lights (white bar), and corresponding relative PAR values measured with Turtle_6 sensors (ratio of incident light = PAR of the sector #*i*/PAR of sector #1) under lamp lighting during the night (black bars). (e) Inset: representation of the six PAR sensors of the Turtle_6. Error bars indicate s.d.

(see the ‘Materials and methods’ section for details). Note that vertical variability was not considered in either the growth chamber given the low height of the *A. thaliana* plants or in the glasshouse because the modifications in directional fluxes measured at the two different heights were negligible in the subplot considered. Thus, the simulations were computed based on characterisations at the soil level.

Light interception was computed in all situations using a light balance model applied to 3D virtual plants

Three-dimensional virtual plants were simulated on a daily basis from plant emergence to the end of plant leaf expansion from measurements carried out on organ growth, development, shape and orientation. The geometry of these 3D virtual plants differed slightly among the genotypes of *A. thaliana* and sunflower, whereas the growth and development of their individual phytomers varied greatly among treatments (data not shown).

The architectural model accurately simulated plant growth and development at the organ and whole-plant levels. Fits of observed data for organ number and dimensions were satisfactorily integrated at the whole-plant level such that the projected total leaf area of *A. thaliana* plants was adequately simulated throughout the plant development period ($y = 0.994 x$), with a correlative coefficient of determination (r^2) between observed and simulated values of 0.908 and mean simulation errors, estimated by CVe, of less than 0.2 (Fig. 5a). In sunflower, the integration of individual organ growth and development resulted in simulations of LAI (Fig. 5b) that correlated closely with observed values ($y = 0.975 x$, $r^2 = 0.999$, CVe = 0.053). Similar results were obtained *a posteriori* when using only half the measurements to compute the fitting parameters used as model inputs, thus suggesting that less frequent measurements can be used to build dynamic 3D virtual plants.

The MMR light calculation model was tested in the growth chamber, in the glasshouse and in the field (Fig. 6). In artificial environments, directional light fluxes were calculated from computed values obtained from measurements in the middle of each subplot. The simulated values were closely correlated with

measurements carried out at other locations within each subplot, for each direction (linear fittings with slopes between 0.97 and 1.01, $r^2 > 0.75$ and CVe < 0.23), thus indicating that the model accurately reproduced the directional light environment of the subplot. In the field, directional light fluxes were simulated based on measurements of incident PAR only. The simulated data were closely related to the measurements obtained with the Turtle device (Fig. 6, inset).

Plant light balance simulations were assessed for plants grown in canopy under natural conditions where measurements of overall light interception by the canopy were possible (Fig. 7). The simulated and measured fractions of intercepted PAR were compared for the Albena and Heliasol hybrids and gave consistent results ($y = 0.996 x$, $r^2 = 0.988$, CVe = 0.05). Evaluation of the model was also carried out at the organ level using mature canopy plants with leaf blades cut such that only the stem, the petioles and the capitulum remained. The fraction of PAR intercepted by these defoliated plants was 0.3 and did not significantly differ from the simulated data (0.33).

The virtual plant approach enabled estimation of light interception where classical approaches are inefficient

The 3D virtual plants coupled with the MMR light model considered the mutual shading of organs from plant emergence until the end of plant leaf expansion. In sunflower, changes in RLI over thermal time showed a similar pattern in each experiment (Fig. 8). First, RLI decreased for $\sim 200^\circ\text{Cd}$ as the leaves expanded, causing mutual shading. RLI then increased for 200°Cd as the stem began to elongate, moving the leaves away from each other. Finally, RLI decreased again until the end of leaf expansion because the stem stopped elongating, while the expansion of the largest leaves increased leaf density and self-shading. Characteristic values for this pattern varied between the different situations. For example, isolated sunflower plants at maturity showed a high RLI value of $\sim 70\%$, whereas plants grown in canopy presented more overlapping leaves and the RLI decreased to 15%. RLI values also differed over time for the different experiments and treatments, illustrating the advantages of an architectural approach. RLI was higher in *A. thaliana* than in

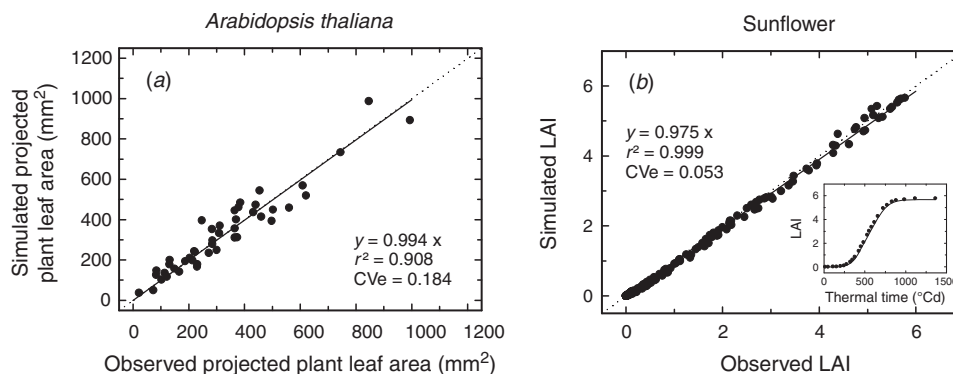


Fig. 5. Test of the 3D architectural model: comparison of simulated versus observed values for (a) projected plant leaf area in *Arabidopsis thaliana* and (b) leaf area index (LAI) in sunflower. Data are derived from different experiments, light treatments, stages and genotypes. Inset, LAI of Albena plants over thermal time since emergence under the control treatment used in Experiment S4.

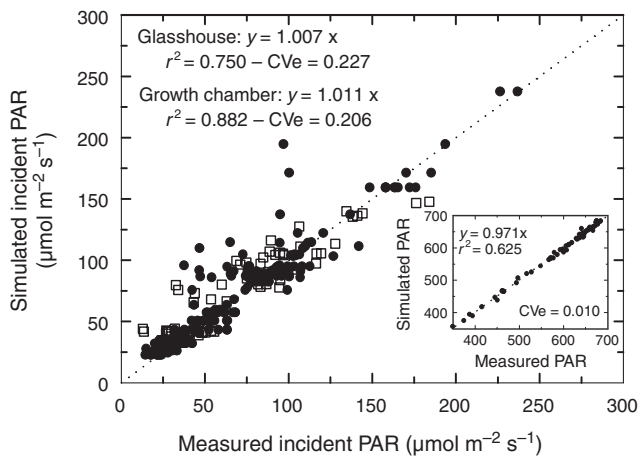


Fig. 6. Test of the radiative model: comparison of simulated versus observed incident PAR for different faces of the Turtle_6 (Fig. 3b) in the growth chamber (●) and glasshouse (□) and for the different faces of the Turtle_16 (Fig. 3a) in the field (inset). In the growth chamber and glasshouse, the simulated data were based on incident PAR and on measurements carried out in the middle of the subplot for each treatment; the data were compared to measurements carried out at different locations within the subplot. In the field, the data were simulated from incident light with MMR accounting for the sun position and the sky brightness. Dots represent the 1 : 1 line.

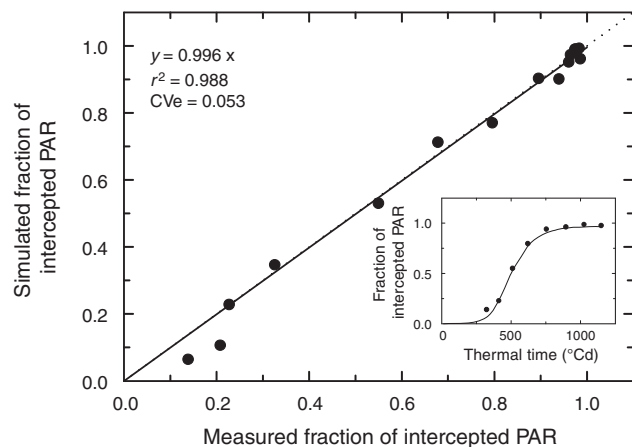


Fig. 7. Test of the integrated model coupling the architectural and radiative models: comparison of simulated versus observed data for the fraction of intercepted light in the sunflower genotypes Albena and Heliasol in Experiment S5. Dots represent the 1 : 1 line. Inset, change in the fraction of intercepted light over thermal time since emergence for Albena; points, observed data; line, simulated data.

sunflower as only a few leaves of the rosette were shaded (Figs 2 and 8a). However, no clear pattern over time was observed in the different experimental situations, supporting the pertinence of the proposed approach to estimate light interception in this species as well.

The use of 3D virtual plants to estimate light absorption was compared with the classical approach of the Beer–Lambert law (Fig. 9). Note that the coefficient of extinction (k) was determined

by a standard method, from direct measurements of LAI and light interception efficiency carried out in the field at normal density (Experiment S5). For sunflower cultivated in the field at normal density (all the treatments of Experiments S4 and 5; Fig. 9g, h), the two approaches gave similar results ($PAR_{a3D} = 1.069 PAR_{aBeer}$, $r^2 = 0.70$, $CVe = 0.024$). However, the Beer–Lambert law underestimated PAR absorption during early crop development, for the first 300°Cd following plant emergence (Fig. 9h, inset). Application of the Beer–Lambert law to a sunflower canopy cultivated in a glasshouse also appeared to be poor, probably owing to the marked heterogeneity in directional light and the low-density canopy (Fig. 9e, f). In these cases, estimations based on the Beer–Lambert law were up to 10-fold lower or threefold higher than estimations based on the 3D approach. Application of the Beer–Lambert law to isolated plants underestimated PAR absorption because more light reaches these plants than canopy plants for which the coefficient of extinction (k) was estimated (Fig. 9c, d).

The PAR absorption calculated by the Beer–Lambert law was also tested for isolated rosette *A. thaliana* plants in the growth chamber (Fig. 9a, b). As the coefficient of extinction (k) for these rosette plants could not be estimated from direct measurements it was computed from the 3D-based approach. A coefficient of extinction of 0.94 was calculated for the Columbia genotype based on data derived from all the conditions investigated in the present study. This value is consistent with the marked plagiotropy of the *A. thaliana* rosette. Under such conditions, the Beer–Lambert law very accurately calculated the PAR absorbed by plants ($PAR_{a3D} = 1.000 PAR_{aBeer}$, $r^2 = 0.998$, $CVe = 0.068$). However, k varied among the genotypes. Had the PAR absorbed by plants of the *rot3-1* mutant been calculated using the Columbia extinction coefficient, the value would have been underestimated by ~50%. The coefficients for the six other genotypes studied were similar to the coefficient determined for Columbia, but *rot3-1* had a k of 0.61. It is noteworthy that incident light here was spatially homogenous because of nets added in the subplots of the growth chamber (either fine-meshed or darker shading nets depending on the treatment). Variations observed in directional light fluxes among the treatments were not taken into account by the Beer–Lambert law, but their consequences were probably negligible here because leaves of *A. thaliana* remain close to the soil and are mostly horizontal.

Another approach commonly used in rosette plants to calculate light interception is to consider that light interception is proportional to plant leaf area. This method gave satisfactory results for Columbia, the standard *A. thaliana* genotype (Fig. 9a, b, $PAR_{a3D} = 1.092 PAR_{aBeer}$, $r^2 = 0.997$, $CVe = 0.094$). When applied to genotypes with contrasting architectures or leaf development, this method resulted in differences of 6–15% with respect to the 3D-based approach for seven of the eight genotypes tested (Fig. 10). In *rot3-1*, this approach led to a 50% under-estimation with respect to the 3D-based approach. Furthermore, the precision of this method varied with plant development and light conditions owing to changes in relative blade irradiance (Figs 8a and 11), thus underlining the advantages of the 3D virtual plant approach for studies on light responses in *A. thaliana*.

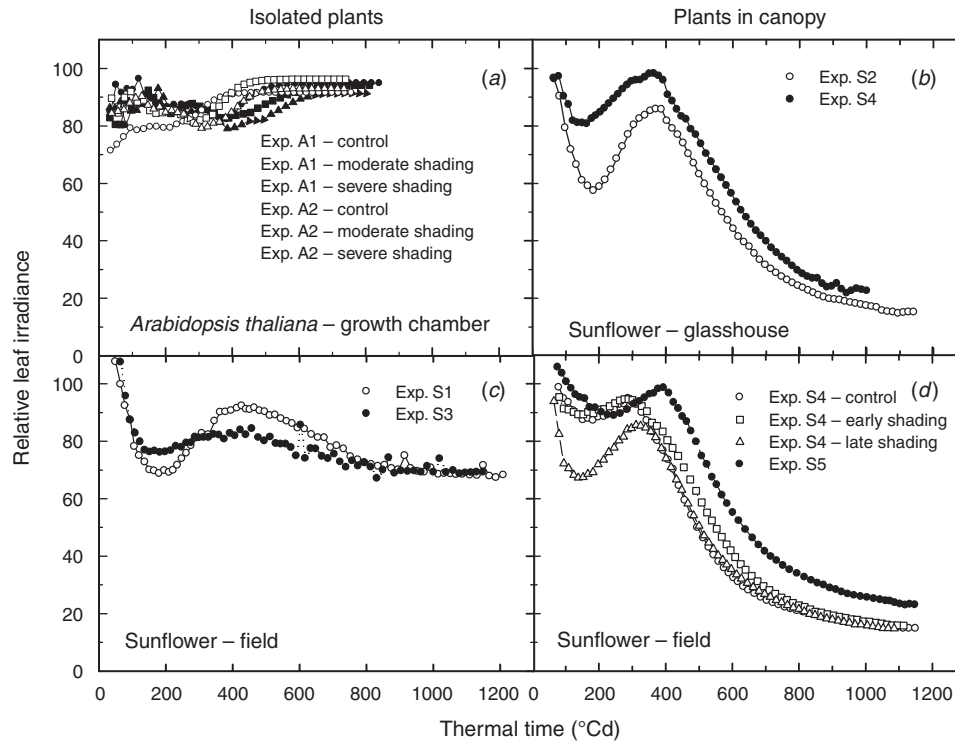


Fig. 8. Change in the relative irradiance of blades over thermal time from emergence until the end of plant leaf expansion in *Arabidopsis thaliana* (ecotype Columbia) and sunflower (hybrid Albena). Plants were grown under artificial (first row: *a, b*) or natural environments (second row: *c, d*), and as isolated plants (first column: *a, c*) or in canopy (second column: *c, d*). For better clarity, only data from Experiments A1 and A2 are shown in (*a*). The sunflower data were adapted from Rey *et al.* (2008).

Discussion

Estimating radiative microclimate in artificial environments

Although growth chambers and glasshouses are designed to minimise environmental heterogeneity, the light climate within these artificial environments is highly heterogeneous (Fig. 4). According to their manufacturers, environmental control systems in growth chambers monitor climatic factors such as temperature and hygrometry. Plants are nevertheless very sensitive to variations in environmental conditions in their immediate vicinity (e.g. Chelle 2005). For instance, even a 2°C difference in air temperature, as commonly observed in growth chambers, will affect plant photosynthesis and development (Boonen *et al.* 2002) and might dissimulate phenotypic differences between two genotypes. Heterogeneity is extreme when considering the light climate. To our knowledge, no existing growth chamber can be considered as homogeneous in terms of incident and directional light distribution. Similar problems occur in glasshouses, where light heterogeneity arises from: (i) local shading of plants by building structures; (ii) light climate variation over time owing to the interaction of daily and seasonal sun course with the glasshouse structures; (iii) artificial lighting (if needed); and (iv) plants that are usually sparsely grown. For all these reasons, the Beer–Lambert law cannot be applied in these situations to estimate light interception (Fig. 9*e, f*).

By contrast, 3D virtual plants placed in a virtual plot that reproduces the light environment can be used to estimate light

interception in such situations. In most cases, 3D light models consider only an isotropic sky (Hanan and Bégue 1995; Chelle and Andrieu 1998; Sinoquet *et al.* 1998). Anisotropic sky effects have been accounted for in the MMR model (Dauzat *et al.* 2001), and recently in the DSHP model (Wang *et al.* 2006), by assimilating incident radiation from a set of directional point-light sources. These models enable simulation in artificial environments, such as growth chambers and glasshouses, provided that data can be collected on the directional patterns. In the present study, 3D virtual plants were coupled with the MMR light model to simulate a broad range of experimental situations.

Accurate estimations of the light climate were possible in the present study because the developed method accounted for: (i) artificial lighting and wall reflection in the growth chamber; and (ii) for sunlight, the impact of building structures on this sunlight, and artificial lighting provided by lamps in the glasshouse. Furthermore, detailed characterisation of the environments, and the addition of shading nets where required, allowed us to work in subplots with homogeneous incident light. In these subplots, the directional light fluxes differed depending on the considered direction, but were homogeneous for different positions across the experiment when considering a single direction.

Given the specificity of the growth chamber or glasshouse, the lighting system (type of light, number, disposition, age) and the

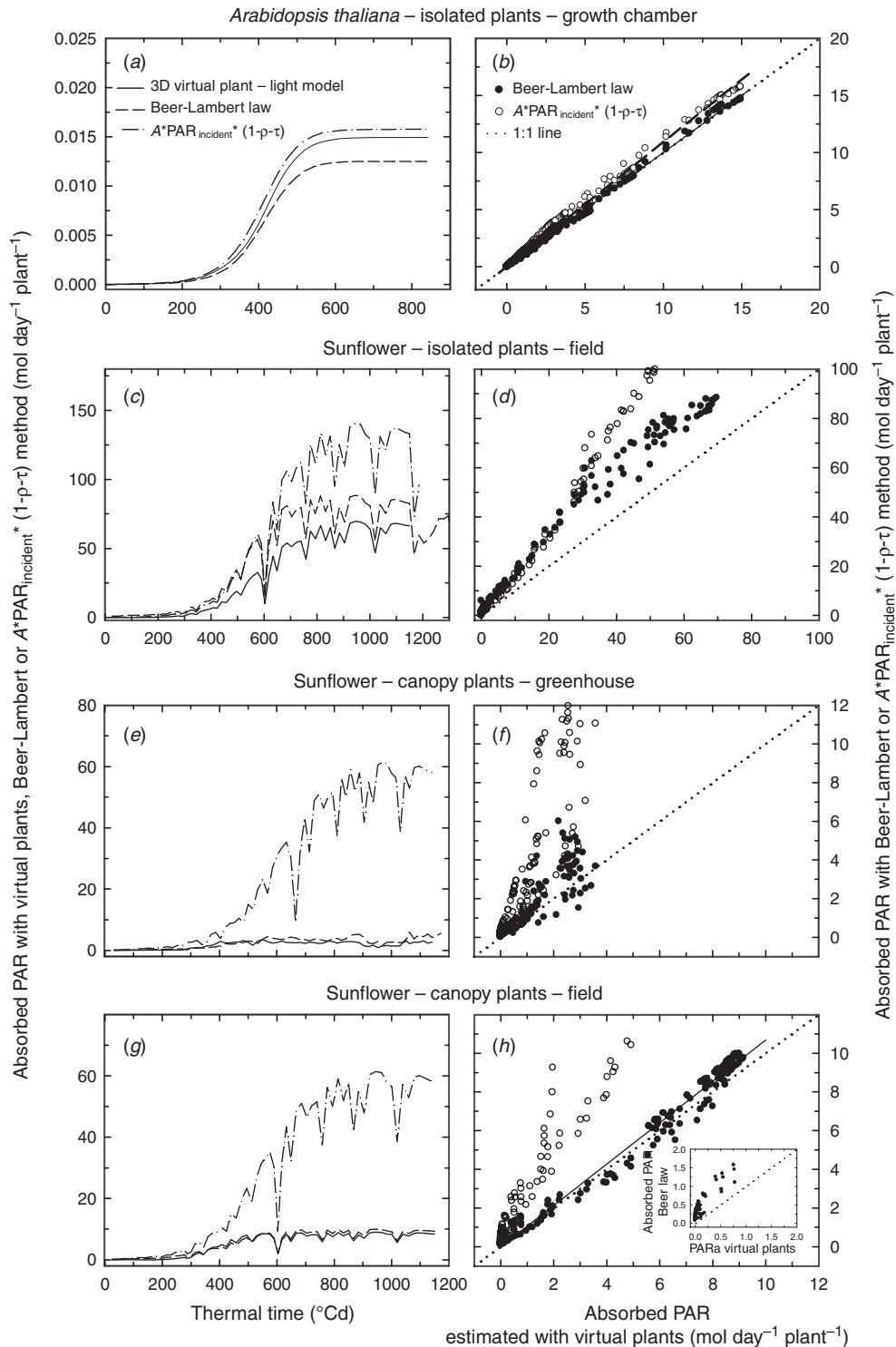


Fig. 9. Comparison of the different approaches used to estimate the amount of light absorbed by plants in various situations for *Arabidopsis thaliana* (ecotype Columbia) and sunflower (hybrid Albena): the estimation using 3D virtual plants coupled with the MMR light model (solid line) was compared with the estimation obtained by the Beer–Lambert law (dashes, ●) and with the estimation provided from the product of plant leaf area (A) by incident PAR ($\text{PAR}_{\text{incident}}$) corrected by a scattering coefficient ($1-p-\tau$) (dash-dot-dash, ○). The comparison was made for isolated *A. thaliana* plants grown in (first row: *a, b*) growth chamber, (second row: *c, d*) isolated sunflower plants grown in the field, (third row: *e, f*) canopy plants of sunflower grown in a glasshouse and (fourth row: *g, h*) canopy plants of sunflower grown in the field. Data are presented over thermal time since emergence (first column: *a, c, e, g*) for the control treatment used in (*a*) Experiment A2, (*c*) Experiment S4, (*e*) Experiment S1 and (*g*) the control treatment in Experiment S4. Data from all treatments are presented versus the estimation based on 3D virtual plants (second column: *b, d, f, h*), where the 1 : 1 line is represented by dots. (*h*) Insert, data corresponding to the early developmental stage (first 300 °Cd following plant emergence).

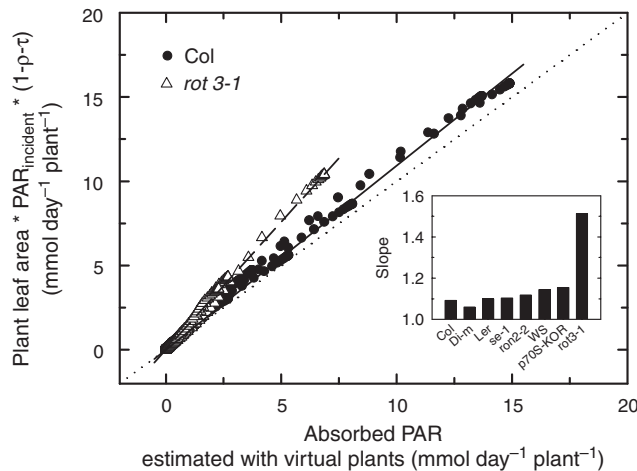


Fig. 10. Absorbed PAR estimated using the 3D virtual plant approach versus absorbed PAR estimated from the product of plant leaf area by incident radiation ($PAR_{incident}$) corrected by a scattering coefficient ($1-p-t$) for different genotypes of *Arabidopsis thaliana*. For better clarity only two genotypes are shown: Columbia (●) and its mutant *rot3-1* (△). Inset: Slope, for the eight genotypes, of the linear relationship between absorbed PAR estimated from the product of plant leaf area by incident radiation and the scattering coefficient and absorbed PAR estimated using the virtual plant approach.

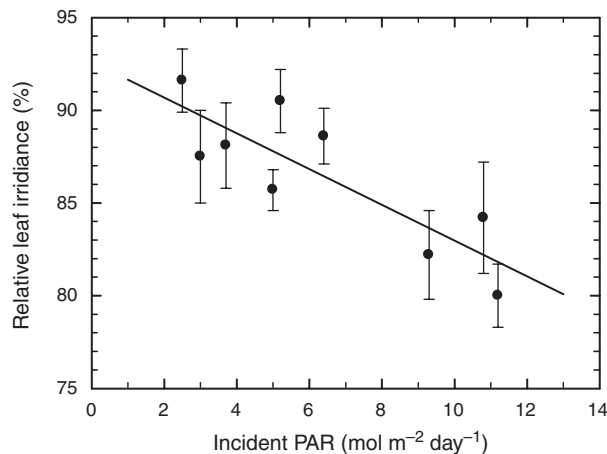


Fig. 11. Relative irradiance of blade versus incident PAR in *Arabidopsis thaliana*, ecotype Columbia. Mean of the daily values from emergence to the end of rosette expansion. Error bars indicate confidence limits at $P=0.05$.

season (for glasshouse experiments), each treatment was considered as a unique radiative system. These radiative systems can be characterised either by measurement of the radiative climate, as proposed here, or by modelling the complete system surrounding the experiment. The method used in the present study could be further developed by designing directional light sensors that would measure direct light instead of hemispherical fluxes, and for various wavelengths. WiFi technology could assist with data collection and energy supply. The second approach consists of modelling all radiative interactions among light sources, materials and plants

for a given experimental device (Chelle *et al.* 2007b). This should allow simulation of light interception in any heterogeneous environment and would be particularly useful for modelling the radiative environment of tall plants in growth chambers, where plants and external structures interact. However, this method might require complex description of the 3D structures (e.g. building structures and light sources) and the parameterisation of their optical properties, which would be difficult in complex environments such as glasshouses. The two approaches are complementary and should both be taken into account when examining the effect of light on plant development and physiology. Furthermore, these methods should be extended to cover the entire solar spectrum, to account for red:far red (Chelle *et al.* 2007a) and blue light effects, and to better estimate the energy balance that depends greatly on the level of infrared radiation.

Model contribution to research investigations

Using 3D virtual plants coupled with the MMR light model presents several advantages over classical approaches. First, as illustrated in the present study, applications are possible in artificial environments and this might be of interest in horticulture and for research studies on plant physiology. Second, the 3D virtual plants used in the present study reproduced the different plant organs. Therefore, the model can be used to calculate the light intercepted at the organ level (Rey *et al.* 2008), which is advantageous when estimating other complex physiological variables, such as photosynthesis, that are greatly affected by the local microclimate (Rapidel *et al.* 1999; Franck *et al.* 2005). Third, this approach can also be used to estimate the impact of changes in plant architecture on light interception (Louarn *et al.* 2008; Rey *et al.* 2008). For example, the increase in petiole length caused by our severe shading led to an almost 10% increase in light interception efficiency in *A. thaliana*, and this was only slightly reduced by a change in leaf shape (1% impact). Fourth, the model can be used to compare the light intercepted by plants at different development stages and in various situations because it accounts for the architectural responses of plants to their environment. By contrast, the Beer–Lambert law was designed for well-developed crops grown in open fields. The results presented here illustrate that, with the same extinction coefficient (k) over time and in different environments, the Beer–Lambert law is not suitable for the early period of plant growth or for isolated sunflower plants (Fig. 9c, d, h, inset). In such situations, physical measurements of light interception are also difficult. Thus, the model can be particularly useful for investigating processes related to the light intercepted during early development, for example, structural and functional plant responses to an early stress (Louarn *et al.* 2008) or for the light response of leaf expansion in dicotyledonous plants, which is very sensitive to the light intercepted during the first exponential phase of leaf expansion (Granier and Tardieu 1999; Chenu *et al.* 2005). It is noteworthy that in the particular case of *A. thaliana*, both the Beer–Lambert law and the method based on multiplication of plant area by incident light gave an accurate estimation of intercepted light for both artificial conditions and different shading treatments (Fig. 9b). However, *A. thaliana* are rosette plants and only

capture a small proportion of the directional light. The 3D virtual plant modelling was nevertheless useful to evaluate these classical methods in such particular conditions. The models further revealed that the fraction of intercepted light increased in shaded plants (Fig. 11).

Several methods are currently available to generate 3D virtual plants and calculate their light climate. 3D virtual plants can be built from either direct measurements taken using a 3D digitiser (e.g. Sinoquet *et al.* 1998), statistical distributions of parameters describing organ shapes and positions (de Reffye *et al.* 1988; España *et al.* 1998; Louarn *et al.* 2007) or plant growth simulations (Mech and Prusinkiewicz 1996; Fournier and Andrieu 1998, 1999; Chenu *et al.* 1999, 2005). The generation of 3D virtual plants, particularly those growing over time, still requires a substantial number of parameters. In our case, we demonstrated that fewer measurements would have been sufficient to parameterise the architectural model, without any significant impact on the results. Further simplifications of such models might also be possible by considering stable relationships between phytomer ranks or stable plant responses to environmental factors (e.g. Tardieu 2003; Chenu *et al.* 2005). Combining architectural models with crop models that simulate plant growth and development at the organ level (Chenu *et al.* 2008) could be of particular interest to simulate plant development in response to the environment using only a small number of parameters. With regard to light models, several methods have been proposed to simulate light scattering in virtual plots. Radiosity (Soler *et al.* 2003) and ray-tracing (Allen *et al.* 2005) depict comprehensively radiative transfers, but are time consuming. Adaptations such as nested radiosity (Chelle and Andrieu 1998) or the quasi-Monte Carlo method (Keller 1996) might nevertheless reduce the computation time. The MMR model further simplifies the system and performs simulations in a shorter computation time (several seconds to simulate the light balance in a sunflower field) with only a standard computer configuration. This model was suitable for calculating canopy light balance throughout crop development in all the tested environments.

A model to compare genotypes

When applicable, both the 3D-based model and classical approaches can be used to estimate the light intercepted by various genotypes, provided that the plant architecture is properly described. To account for genotypic differences, methods based on plant leaf area generally use a single genotype-specific parameter that is constant throughout plant development and between the different situations. Using this method to compare the light intercepted by different genotypes is quicker than using the 3D-based approach, but comparisons are limited to conditions in which these methods are applicable. The advantage of the 3D-based method is that it allows investigation of the application range of these methods (environmental conditions, location, developmental stage, genotype), and helps to parameterise these methods for various genotypes. This is of particular interest when direct measurements are difficult, as illustrated in the present study with isolated *A. thaliana* plants grown in a growth chamber (Figs 9a, b and 10).

Another limitation of classical approaches when they are used to compare genotypes is that they do not account for genotype–environment interactions. Therefore, such approaches should only be used in similar environmental conditions to those used for their parameterisation (e.g. estimation of k for the Beer–Lambert law for a given genotype, density and environment). Given that plants show great structural plasticity to their environment, the 3D-based method would appear to be more appropriate than classical methods for comparing genotypes when plants are grown in different situations. Therefore, the 3D-based approach should be preferred when comparing genotypic responses to environmental factors that affect plant architecture (Chenu *et al.* 2007).

Three-dimensional virtual plants combined with a light model can also be used to analyse genetic variability in terms of plant architecture and intercepted light efficiency. The two sunflower hybrids examined in the present study showed similar plant leaf areas, but Heliasol absorbed more light than Albena, clearly illustrating how organ arrangement impacts on light interception. The past 30 years of sunflower breeding have led to the selection of germplasms with different architectures and increased interception of light per unit leaf area (Debaeke *et al.* 2004). In addition, architectural variables have recently been found to be highly heritable (Triboi *et al.* 2004). Therefore, the 3D-based approach appears to offer great promise for analysing the relative contribution of architectural traits in various genotypes and gives plant breeders new selection criteria to improve light capture.

Acknowledgements

We thank M. Van Lijsebettens, J.L. Micol and S. Vernhettes for seeds of *se-1*, *ron2-2* and *p70S-KOR*, respectively. We also thank G. Chenu and F. Painparay for their support, and S.C. Chapman and the anonymous reviewers for improving the manuscript. This work was partly funded by PROMOSOL in connection with the PRODUCTIVITE I and II projects and by the European Community Human Potential Program (HPRB-CT-2002-00267) as part of the DAGOLIGN Research Training Network.

References

- Allen MT, Prusinkiewicz P, DeJong TM (2005) Using L-systems for modeling source–sink interactions, architecture and physiology of growing trees: the L-PEACH model. *New Phytologist* **166**, 869–880. doi: 10.1111/j.1469-8137.2005.01348.x
- Anonymous (1992) 'LAI-2000 plant canopy analyser. Operating manual.' (LICOR: Lincoln)
- Auclair D, Barcezi JF, Borne F, Etienne M (2001) Assessing the visual impact of agroforestry management with landscape design software. *Landscape Research* **26**, 397–406. doi: 10.1080/01426390120090166
- Barcezi JF, Rey H, Caraglio Y, de Reffye P, Barthélémy D, Dong QX, Fourcaud T (2008) AmapSim: an integrative whole-plant architecture simulator based on botanical and environmental plasticity knowledge. *Annals of Botany* **101**, 1125–1138. doi: 10.1093/aob/mcm194
- Boonen C, Samson R, Janssens K, Pien H, Lemeur R, Berckmans R (2002) Scaling the spatial photosynthesis from leaf to canopy in a plant growth chamber. *Ecological Modelling* **156**, 201–212. doi: 10.1016/S0304-3880(02)00171-0
- Chelle M (2005) Phylloclimate or the climate perceived by individual plant organs: What is it? How to model it? What for? *New Phytologist* **166**, 781–790. doi: 10.1111/j.1469-8137.2005.01350.x

- Chelle M, Andrieu B (1998) The nested radiosity model for the distribution of light within plant canopies. *Ecological Modelling* **111**, 75–91. doi: 10.1016/S0304-3800(98)00100-8
- Chelle M, Andrieu B (1999) Radiative models for architectural modeling. *Agronomie* **19**, 225–240. doi: 10.1051/agro:19990304
- Chelle M, Evers JB, Combes D, Varlet-Grancher C, Vos J, Andrieu B (2007a) Simulation of the three-dimensional distribution of the red : far-red ratio within crop canopies. *New Phytologist* **176**, 223–234. doi: 10.1111/j.1469-8137.2007.02161.x
- Chelle M, Renaud C, Delepoulle S, Combes D (2007b) Modeling light phylloclimate within growth chambers. In 'Proceedings of the 5th International Workshop on Functional-Structural Plant Models. Napier, New Zealand.' (Eds P Prusinkiewicz, L Hanan, B Lane) pp. 57-1–57-4. (Print Solutions Hawke's Bay Limited: Napier, New Zealand)
- Chenu K, Franck N, Dauzat J, Barczy JF, Rey H, Lecoeur J (2005) Integrated responses of rosette organogenesis, morphogenesis and architecture to reduced incident light in *Arabidopsis thaliana* results in higher efficiency of light interception. *Functional Plant Biology* **32**, 1123–1134. doi: 10.1071/FP05091
- Chenu K, Franck N, Lecoeur J (2007) Simulations of virtual plants reveal a role for *SERRATE* in the response of leaf development to light in *Arabidopsis thaliana*. *New Phytologist* **175**, 472–481. doi: 10.1111/j.1469-8137.2007.02123.x
- Chenu K, Chapman SC, Hammer GL, McLean G, Tardieu F (2008) Short term responses of leaf growth rate to water deficit scale up to whole-plant and crop levels. An integrated modelling approach in maize. *Plant, Cell & Environment* **31**, 378–391. doi: 10.1111/j.1365-3040.2007.01772.x
- Cookson SJ, Granier C (2006) A dynamic analysis of the shade-induced plasticity in *Arabidopsis thaliana* rosette leaf development reveals new components of the shade-adaptative response. *Annals of Botany* **97**, 443–452. doi: 10.1093/aob/mcj047
- Dauzat J, Eroy MN (1997) Simulating light regime and intercrop yields in coconut based farming systems. *European Journal of Agronomy* **7**, 63–74. doi: 10.1016/S1161-0301(97)00029-4
- Dauzat J, Rapidel B, Berger A (2001) Simulation of leaf transpiration and sap flow in virtual plants: model description and application to a coffee plantation in Costa Rica. *Agricultural and Forest Meteorology* **109**, 143–160. doi: 10.1016/S0168-1923(01)00236-2
- Dauzat J, Martin P, Luquet D, Clouef P (2008) Using virtual plants for analysing the light foraging efficiency of cotton crop at low density. *Annals of Botany* **101**, 1153–1166.
- de Reffye P, Edelin C, Françon J, Jaeger M, Puech C (1988) Plant models faithful to botanical structure and development. In 'Proceedings of SIGGRAPH '88, Atlanta, Georgia, 1–5 August 1988.' (Ed. J Dill). *Computer Graphics* **22**, 151–158. doi: 10.1145/378456.378505
- Debaeke P, Triboi AM, Vear F, Lecoeur J (2004) Crop physiological determinants of yield in old and modern sunflower hybrids. In 'Proceedings of the 16th International Sunflower Conference. ISA, Fargo, ND, USA'. (Ed. ISA) pp. 267–273. (Fargo: ND, USA)
- den Dulk J (1989) 'The interpretation of remote sensing, a feasibility study.' (Wageningen University: Wageningen)
- España M, Baret F, Chelle M, Aries F, Andrieu B (1998) A dynamic model of maize 3D architecture: application to the parameterisation of the clumpiness of the canopy. *Agronomie* **18**, 609–626. doi: 10.1051/agro:19981001
- Fournier C, Andrieu B (1998) A 3D architectural and process-based model of maize development. *Annals of Botany* **81**, 233–250. doi: 10.1006/ambo.1997.0549
- Fournier C, Andrieu B (1999) ADEL-maize: an L-system based model for the integration of growth processes from the organ to the canopy. Application to regulation of morphogenesis by light availability. *Agronomie* **19**, 313–327. doi: 10.1051/agro:19990311
- Franck N, Vaast P, Génard M, Dauzat J (2005) Soluble sugars mediate sink feedback down-regulation of leaf photosynthesis in field-grown *Coffea arabica*. *Tree Physiology* **26**, 517–525.
- Granier C, Tardieu F (1998) Is thermal time adequate for expressing the effects of temperature on sunflower leaf development? *Plant, Cell & Environment* **21**, 695–703. doi: 10.1046/j.1365-3040.1998.00319.x
- Granier C, Tardieu F (1999) Leaf expansion and cell division are affected by reducing absorbed light before but not after the decline in cell division rate in the sunflower leaf. *Plant, Cell & Environment* **22**, 1365–1376. doi: 10.1046/j.1365-3040.1999.00497.x
- Granier C, Massonnet C, Turc O, Muller B, Chenu K, Tardieu F (2002) Individual leaf development in *Arabidopsis thaliana*: a stable thermal-time-based programme. *Annals of Botany* **89**, 595–604. doi: 10.1093/aob/mcf085
- Guilioni L, Lhomme JP (2006) Modelling the daily course of capitulum temperature in a sunflower canopy. *Agricultural and Forest Meteorology* **138**, 258–272. doi: 10.1016/j.agrformet.2006.05.010
- Guyot G (1990) Optical properties of vegetation canopies. In 'Application of remote sensing in agriculture.' (Eds MD Steven, JA Clark) pp. 19–44. (Butterworths: London)
- Hanan NP, Bégue A (1995) A method to estimate instantaneous and daily intercepted photosynthetically active radiation using a hemispherical sensor. *Agricultural and Forest Meteorology* **74**, 155–168. doi: 10.1016/0168-1923(94)02196-Q
- Jonckheere I, Flock S, Nackaerts K, Muys B, Coppin P, Weiss M, Baret F (2004) Review of methods for in situ leaf area index determination: Part I. Theories, sensors and hemispherical photography. *Agricultural and Forest Meteorology* **121**, 19–35. doi: 10.1016/j.agrformet.2003.08.027
- Kasanga H, Monsi M (1954) On the light transmission of leaves, and its meaning for the production of dry matter in plant communities. *Japanese Journal of Botany* **14**, 304–324.
- Keller A (1996) Quasi-Monte Carlo methods in computer graphics: the global illumination problem. *Lectures in Applied Mathematics* **32**, 455–469.
- Lecoeur J, Ney B (2003) Change with time in potential radiation-use efficiency in field pea. *European Journal of Agronomy* **19**, 91–105. doi: 10.1016/S1161-0301(02)00019-9
- Louarn G, Guédon Y, Lecoeur J, Lebon E (2007) Quantitative analysis of the phenotypic variability of shoot architecture in two grapevine cultivars (*Vitis vinifera* L.). *Annals of Botany* **99**, 425–437. doi: 10.1093/aob/mcl276
- Louarn G, Chenu K, Fournier C, Andrieu B, Giauffret C (2008) Relative contributions of light interception and radiation use efficiency to the reduction of maize productivity under cold temperatures. *Functional Plant Biology* **35**, 885–899.
- Measures M, Weinberger P, Baer H (1973) Variability of plant growth within controlled-environment chambers as related to temperature and light distribution. *Canadian Journal of Plant Science* **53**, 215–220.
- Mech R, Prusinkiewicz P (1996) Visual models of plants interacting with their environment. In 'Proceedings of SIGGRAPH 96, New Orleans, LA, 4–9 August 1996.' pp. 397–410. Available at <http://algorithmicbotany.org/papers/enviro.sig96.pdf> [Verified 8 September 2008]
- Monteith JL (1977) Climate and efficiency of crop production in Britain. *Philosophical Transactions of the Royal Society of London. Series B, Biological Sciences* **281**, 277–294. doi: 10.1098/rstb.1977.0140
- Rapidel B, Dauzat J, Berger A (1999) Application of a mock-up based transpiration and photosynthesis model on a coffee plantation in Costa Rica. In 'Multi-strata agroforestry systems with perennial crops. International Symposium on Multi-Strata Agroforestry Systems with Perennial Crops. Turrialba, Costa Rica, CATIE.' (Eds F Jiménez, J Beer) pp. 198–203. (CATIE: Turrialba, Costa Rica)

- Rey H, Dauzat J, Chenu K, Barczi JF, Dosio GAA, Lecoeur J (2008) Using a 3-D virtual sunflower to simulate light capture at organ, plant and plot levels: contribution of organ interception, impact of heliotropism and analysis of genotypic differences. *Annals of Botany* **101**, 1139–1151. doi: 10.1093/aob/mcm300
- Rinaldi M, Lsavio N, Flagella Z (2003) Evaluation and application of the Oilcrop-Sun model for sunflower in southern Italy. *Agricultural Systems* **78**, 17–30. doi: 10.1016/S0308-521X(03)00030-1
- Röhrig M, Stützel H, Alt C (1999) A three-dimensional approach to modeling light interception in heterogeneous canopies. *Agronomy Journal* **91**, 1024–1032.
- Sadras VO, Milroy SP (1996) Soil-water thresholds for the responses of leaf expansion and gas exchange: a review. *Field Crops Research* **47**, 253–266. doi: 10.1016/0378-4290(96)00014-7
- Sinoquet H, Thanisawanyangkura S, Mabrouk H, Kasemsap P (1998) Characterization of the light environment in canopies using 3D digitising and image processing. *Annals of Botany* **82**, 203–212. doi: 10.1006/anbo.1998.0665
- Sinoquet H, Le Roux X, Adam B, Ameglio T, Daudet FA (2001) RATP: a model for simulating the spatial distribution of radiation absorption, transpiration and photosynthesis within canopies: application to an isolated tree crown. *Plant, Cell & Environment* **24**, 395–406. doi: 10.1046/j.1365-3040.2001.00694.x
- Soler C, Sillion FX, Blaise F, de Reffÿe P (2003) An efficient instantiation algorithm for simulating radiant energy transfer in plant models. *ACM Transactions on Graphics* **22**, 204–233. doi: 10.1145/636886.636890
- Tardieu F (2003) Virtual plants: modelling as a tool for the genomics of tolerance to water deficit. *Trends in Plant Science* **8**, 9–14. doi: 10.1016/S1360-1385(02)00008-0
- Triboi AM, Messaoud J, Debaeke P, Lecoeur J, Vear F (2004). Heredity of sunflower leaf characters useable as yield predictors. In 'Proceedings of the 16th International Sunflower Conference, ISA, Fargo, ND, USA.' (Ed. ISA) pp. 517–523. (Fargo: ND, USA)
- Varlet-Grancher C, Gosse G, Chartier M, Sinoquet H, Bonhomme M, Allirand JM (1989) Mise au point: rayonnement solaire absorbé ou intercepté par un couvert végétal. *Agronomie* **9**, 419–439. doi: 10.1051/agro:19890501
- Walter A, Scharr H, Gilmer F, Zierer R, Nagel KA, *et al.* (2007) Dynamics of seedling growth acclimation towards altered light conditions can be quantified via GROWSCREEN: a setup and procedure designed for rapid optical phenotyping of different plant species. *New Phytologist* **174**, 447–455. doi: 10.1111/j.1469-8137.2007.02002.x
- Wang XP, Guo Y, Li BG, Wang XY, Ma YT (2006) Evaluating a three dimensional model of diffuse photosynthetically active radiation in maize canopies. *International Journal of Biometeorology* **50**, 349–357. doi: 10.1007/s00484-006-0032-0

Manuscript received 7 March 2008, accepted 29 July 2008